Quality and Reliability Engineering International

WILEY

RESEARCH ARTICLE OPEN ACCESS

Windowed Mean Drift Exponentially Weighted Moving Average Control Chart for Monitoring Complex Autocorrelated Processes

Jeanette Maria Louw[1] | Jean-Claude Malela-Majika[1] | Kayode Samuel Adekeye[2] | Aamir Saghir[3]

[1]Department of Statistics, Faculty of Natural and Agricultural Sciences, University of Pretoria, Pretoria, South Africa | [2]Office of the Deputy Vice-Chancellor(T&L), University of The Gambia, Serekunda, The Gambia | [3]Department of Statistics, Mirpur University of Science and Technology (MUST), Mirpur, Pakistan

Correspondence: Jean-Claude Malela-Majika (malela.mjc@up.ac.za)

Received: 9 October 2025 | **Revised:** 14 December 2025 | **Accepted:** 15 January 2026

Keywords: autocorrelated data | dynamic data patterns | MD-EWMA | mean drift | windowed out-of-control mitigation | WMD-EWMA

ABSTRACT

In modern manufacturing environments, traditional statistical process control (SPC) methods often struggle with complex, dynamic data patterns, particularly when observations are autocorrelated. Control charts are useful tools used in SPC to detect any significant drift in a process. Thus, there is an increasing interest in improving their detection ability, regardless of the nature and complexity of the data. This paper introduces two new exponentially weighted moving average (EWMA) charts for monitoring mean drifts in a process. The first one is named, mean drift EWMA (MD-EWMA) chart, and the second one, named windowed mean drift EWMA (WMD-EWMA) chart, which is the enhanced version of the MD-EWMA chart. The effectiveness of both charts in detecting moderate and large mean drifts while minimising false positives is explored under different scenarios. Furthermore, the performance of the WMD-EWMA chart is compared with the MD-EWMA, EWMA and CUSUM charts. The comparison results reveal the necessity of a window-based approach in reducing false positives, particularly when specific behavioural patterns are expected. Through extensive simulations and real-world case studies, the WMD-EWMA chart is shown to outperform the MD-EWMA, Shewhart, EWMA, and CUSUM charts by effectively identifying significant mean drifts and reducing false alarms.

1 | Introduction

Statistical process control (SPC) remains a cornerstone of quality management and continuous improvement across various industries. As manufacturing processes become increasingly complex and data-rich, there is a growing need for more sophisticated or advanced monitoring techniques that can adapt to changing conditions and detect process drifts, particularly in the presence of autocorrelated data, where data points exhibit dependency over time; see, for example, Kim et al. [1]. and Xue et al. [2]. Control charts, fundamental tools in SPC, offer a visual representation of process behaviour over time, enabling practitioners to distinguish between a common cause of variation, which is inherent to the process and considered 'in-control' and special cause of variation, which indicates potential issues in the process and is deemed 'out-of-control'. This distinction allows for timely interventions and process optimisations, ensuring consistent quality and performance; see, for example, Montgomery [3], Lima de Mendonca et al. [4]. and Wotango et al. [5].

The pioneering work of Shewhart [6] laid the foundation for control charts designed to detect large drifts in process parameters. However, as manufacturing processes became more refined, the need to detect smaller drifts became apparent. This led to

This is an open access article under the terms of the Creative Commons Attribution License, which permits use, distribution and reproduction in any medium, provided the original work is properly cited.

© 2026 The Author(s). *Quality and Reliability Engineering International* published by John Wiley & Sons Ltd.

the development of the Exponentially Weighted Moving Average (EWMA) control chart by Roberts [7], which excels at detecting small drifts in process parameters due to its weighting structure that emphasises recent observations while still considering past data. In modern process monitoring, new challenges arise due to the autocorrelated nature of many processes. In such cases, data points are not independent and drifts in the process mean or variability are often more cyclic and pronounced. For instance, the temperature of central processing units (CPUs) often shows autocorrelation, with readings being influenced by previous temperatures and exhibiting cyclical patterns due to cooling cycles and workload variations. While the EWMA control chart is widely used in such situations due to its simplicity and ease of interpretation, it lacks sensitivity to large drifts and struggles with autocorrelated data. The EWMA chart's struggle with autocorrelated data stems from its underlying assumption of independence between observations. When applied to autocorrelated processes, EWMA charts often produce an excessive number of false alarms or, conversely, fail to detect genuine process drifts masked by the autocorrelation pattern. This limitation can result in unnecessary process adjustments, wasted resources and missed opportunities for timely interventions (see, Kurtulus et al. [8]).

To address the autocorrelation limitation, fitting a time series model to the data is a common and effective approach. This process generally involves identifying a suitable model structure, such as the autoregressive integrated moving average (ARIMA), estimating the selected model's parameters and using the one-step-ahead prediction errors for monitoring purposes. These prediction errors, being approximately uncorrelated, provide a more reliable basis for process monitoring. This need has led to the development of more sophisticated tools to overcome the autocorrelation challenge, such as the 'approximate EWMA procedure for correlated data' (see, Ramjee et al. [9]). The foundation of the approximate EWMA procedure for correlated data was laid by Montgomery and Mastrangelo [10], who recognised that the traditional EWMA statistic could approximate certain ARIMA models for time-dependent observations. Specifically, this procedure focusses on approximating an ARIMA(0,1,1) process, also known as IMA(1,1). This procedure is referred to as the IMA-EWMA procedure. In this paper, we used the IMA-EWMA procedure to construct a control chart for monitoring autocorrelated processes and the resulting chart is called MD-EWMA chart. The key benefits of this approach include:

i. Optimal forecasting: the MD-EWMA statistic leverages the property that the EWMA statistic provides the optimal one-step-ahead forecast for the IMA(1,1) process. This allows for efficient forecasting without the need for complex ARIMA modelling.
ii. Dynamic control limits: unlike traditional EWMA charts with fixed control limits, the MD-EWMA employs dynamically adjusted limits. This adaptation makes the chart more sensitive to gradual drifts in the process mean, even in the presence of autocorrelation.
iii. Unified framework: the MD-EWMA chart offers a cohesive approach to both monitoring and forecasting, eliminating the need for separate tools or techniques when dealing with autocorrelated data.
iv. Robustness to process drifts: the chart's design allows it to maintain control over processes experiencing slow, steady changes, a common characteristic of autocorrelated processes.
v. Original observation use: by working with original observations rather than residuals, the MD-EWMA chart maintains ease of interpretation for practitioners familiar with traditional control charts.
vi. Other time-series forms: beneficially, other forms of the ARIMA process can be modelled in a MD-EWMA framework, provided the process shows positive correlation and the mean does not change rapidly over time (see, Montgomery [3])

While the MD-EWMA chart represents a significant advancement in handling autocorrelated data, it is not without its limitations. The MD-EWMA's sophisticated approach to managing autocorrelation relies on specific model assumptions, which can present challenges in both implementation and interpretation. This reliance on model assumptions can be particularly problematic when the actual data distribution deviates from these assumptions or when there is significant process variability. In such cases, the MD-EWMA chart tends to produce an excessive number of false alarms, erroneously suggesting that the process is out-of-statistical control when it may be operating within acceptable parameters. For more details on MD-type control charts, readers are referred to Montgomery and Mastrangelo [10], Chen et al. [11], Montgomery [3] and Mou et al. [12].

The high rate of false positives associated with the MD- EWMA chart can have several detrimental effects on process monitoring and quality control efforts. Each false alarm typically triggers unnecessary investigations, leading to wasted time and resources. Moreover, repeated false alarms can undermine confidence in the monitoring system and may desensitise users to the control chart's signals. This desensitisation can result in a 'cry wolf' scenario, where operators might begin to disregard or downplay the importance of signals, potentially missing crucial indicators of genuine process drifts. These limitations underscore the need for further refinement in-control chart methodologies for autocorrelated processes, leading to the development of the windowed mean drift EWMA (WMD-EWMA) chart.

The WMD-EWMA control chart introduces a windowing approach to reduce high false positive rates during large process drifts by operating on the principle of contextual analysis. By considering a window of observations rather than isolated data points, this method provides a more comprehensive view of the process behaviour when certain behaviour is expected. This approach is especially effective at distinguishing genuine mean drift anomalies from temporary fluctuations that could otherwise trigger false alarms.

Various windowing approaches are tailored to suit particular application contexts. Zhao et al. [13]. utilised a window-based method to detect anomalies in social network data, demonstrating the effectiveness of this technique in reducing false positives. Similarly, Wang et al. [14]. presented a windowing mechanism that is specifically designed to detect large mean drifts, further reinforcing the robustness of window-based methods in

maintaining detection precision. This approach is particularly effective at distinguishing between actual drifts and noise in the data. However, there is a notable gap in the research regarding the use of parametric methods within a window-based framework for detecting mean drifts in a process and even fewer studies account for the presence of autocorrelated data in this context.

The remainder of this paper is structured to thoroughly examine the WMD-EWMA control chart, focusing on its enhancements over the MD-EWMA control chart. The paper begins with a mathematical background on the EWMA, MD-EWMA and WMD-EWMA charts. This sets the stage for a detailed exploration of the WMD-EWMA control chart's conceptual framework and its methodological advancements, emphasising its superior ability to detect large mean drifts in autocorrelated data. Following the mathematical foundations, the methodology section introduces the three operational phases of the WMD-EWMA: retrospective, prospective and windowed out-of-control mitigation. Each phase guides the reader for algorithmic purposes, including the mathematical model, parameter selection, control limit setting and the integration of windowed out-of-control mitigation to minimise false positives. Two synthetic datasets and two real datasets are used to compare the performance of the MD-EWMA and WMD-EWMA charts, with evaluation metrics, in-control average run length (ARL_0) and control chart visualisations providing insights into their relative effectiveness. The comparative analysis focusses on detecting large mean drifts in the process mean, especially in autocorrelated data, high- lighting the practical advantages of the WMD-EWMA in various industrial settings. Finally, the paper concludes with a discussion of the findings, offering recommendations for further research and practical implementation. Here the strengths and limitations of the WMD-EWMA chart are addressed, proposing enhancements and future directions to improve its effectiveness in modern process monitoring and quality control.

2 | Mathematical Background

This section examines the progression from EWMA chart to the proposed MD-EWMA chart and establishes the connection to the proposed WMD-EWMA chart. Key terminology and concepts are defined through mathematical reasoning, foundational principles and statistical properties. A comprehensive analysis of each method is provided, ensuring the reader understands their theoretical foundations.

2.1 | The EWMA Control Chart

The traditional EWMA charts, proposed by Roberts [7], are applicable to independent and identically distributed (i.i.d.) observations dependent on time t, say X_t, under the distributional assumption of normality with the in-control mean of μ_0 and in-control variance of σ_0^2. When rational subgroups of size greater than one are encountered, the traditional EWMA charts can be applied to monitor the average of these subgroups over time. The EWMA statistic for individual observation is defined as

$$Z_t = \lambda X_t + (1-\lambda) Z_{t-1}, \tag{1}$$

where λ ($0< \lambda \leq 1$) is the smoothing constant. The initial value Z_0 is typically set to the in-control process mean, μ_0. It is worth noting, when $\lambda = 1$, then Equation (1) reduces to the Shewhart statistic.

The mean and variance of the EWMA statistic defined in Equation (1) are defined by

$$\begin{aligned} &\mu_Z = \mu_0 \\ &\text{and} \\ &\sigma_Z^2 = \sigma_0 \sqrt{\frac{\lambda}{2-\lambda}\left[1-(1-\lambda)^{2t}\right]} \end{aligned} \tag{2}$$

The lower/upper control limits (LCL_t/UCL_t) and centreline (CL) for the EWMA chart are given by

$$\begin{aligned} &LCL_t/UCL_t = \mu_z \pm L\sigma_z \\ &\text{and} \\ &CL = \mu_z, \end{aligned} \tag{3}$$

respectively, where the control limit multiplier L ($L > 0$) is the width of the interval from the centreline.

The EWMA control chart signals an out-of-control condition if the EWMA plotting statistic Z_t falls on or outside the control limits.

2.2 | Mean Drift-EWMA Control Chart

The mean drift control chart is a control chart pattern that indicates a gradual, continuous shift in the process mean, rather than an abrupt one. This is mostly encountered in time-series processes such as autoregressive (AR), moving average (MA), IMA, ARIMA, etc.; see, for example, Mejri et al. [15], Yi et al. [16]. and De Smedt et al. [17].

An IMA (1,1) process is mathematically defined by

$$X_t = X_{t-1} + a_t - \theta a_{t-1}, \tag{4}$$

where a_t are i.i.d. errors, typically called a white noise process, that is assumed to be normally distributed with a zero mean and a variance of σ_E^2, and the parameter θ can be positive or negative and it is usually bounded by -1 and 1. It is clear that the observations X_t at time t are autocorrelated.

The one-step-ahead prediction errors are calculated as

$$E_t = X_t - \hat{X}_t(t-1), \tag{5}$$

where $\hat{X}_t(t-1)$ is the one-step-ahead forecast for time t, made at time $t-1$. By definition of one-step-ahead prediction errors of an IMA(1,1) process, it follows that $a_t = E_t$. Now, by setting a restriction of $\lambda = 1-\theta$ for positive θ that is bounded by 1, the EWMA statistic defined in Equation (1) provides the optimal one-step-ahead forecast for an IMA(1,1) process, which is given by $\hat{X}_t(t-1) = Z_{t-1}$ (see, the proof provided in Appendix A).

The control limits are determined by first calculating the probability of one-step-ahead prediction errors falling within a static threshold and then simplifying this to the probability of the autocorrelated observations fitting within a non-static limit, specifically time-dependent. The process can be expressed through the following equation:

$$P\ (-L\sigma_E \le E_t \le L\sigma_E) = 1-\alpha,$$

then

$$P\ \left(\hat{X}_t\,(t-1) - L\sigma_E \le X_t \le \hat{X}_t\,(t-1) + L\sigma_E\right) = 1-\alpha. \quad (6)$$

Equation (6) can also be written as

$$P\ (Z_{t-1} - L\sigma_E \le X_t \le Z_{t-1} + L\sigma_E) = 1-\alpha. \quad (7)$$

From Equation (7), the lower/upper control limits (LCL_{MD_t}/UCL_{MD_t}) and centreline (CL_{MD_t}) for the MD-EWMA chart become

$$\begin{aligned} &LCL_{MD_t}/UCL_{MD_t} = Z_{t-1} \pm L_{MD}\sigma_E \\ &\text{and} \\ &CL_{MD_t} = Z_{t-1}, \end{aligned} \quad (8)$$

respectively; where L_{MD} is the MD-EWMA chart control limit multiplier and it is set based on prespecified (i.e., nominal) ARL_0. In this paper, the $ARL_0 = 350$ is selected, as this value falls within the typical range used in practice. In manufacturing and process control environments, this threshold corresponds to generating one false out-of-control signal on average every 350 samples when the process is in control (see, Montgomery [3]), striking a practical balance between minimising false alarms to maintain operator confidence in the system and ensuring sufficient sensitivity to detect genuine mean drifts that require corrective action. The variance estimates of the prediction error, σ_E^2, can be estimated in two ways (see, Kurtulus et al. [8].). A time-independent estimate, say $\hat{\sigma}_E^2$, is suitable to use when the variability of X_t is stable. In contrast, a time-dependent estimate, say $\hat{\sigma}_{E_t}^2$, is preferable when the variance of X_t is unstable.

The MD-EWMA control chart signals an out-of-control condition if the MD-EWMA plotting statistic X_t falls on or outside the control limits.

2.3 | Window Mean Drift-EWMA Control Chart

The proposed window mean drift-EWMA (WMD-EWMA) control chart is designed to effectively detect anomalies in autocorrelated data by identifying the initial point of a mean drift while preventing subsequent false alarms from the same underlying change. Building upon the MD-EWMA approach, the WMD-EWMA control chart integrates a windowing mechanism that enhances robustness against noise and substantial mean drifts by temporarily halting anomaly detection for say, W observations following each detected anomaly, effectively mitigating the cascade of false positives that would otherwise occur as the process transitions to its new operating level.

The selection of the window length W requires background knowledge about specific characteristics of the monitored process, as it directly governs the balance between detection responsiveness and false positive control. Shorter windows allow faster detection of subsequent drifts but risk misidentifying post-drift fluctuations as new anomalies, whereas longer windows reduce false positives but may delay the identification of genuine subsequent drifts. For processes where mean drifts occur frequently, shorter windows are preferable to minimise the delay in detecting the next genuine anomaly. Conversely, for processes where drifts are sporadic, longer windows are more appropriate as they provide adequate time for the process to stabilise after each detected anomaly before resuming monitoring. Additionally, processes with high post-drift variance benefit from longer windows that filter out noise and prevent misclassifying natural fluctuations as new anomalies. Section 3.3 provides a more practical discussion of window-length selection.

Let A_t be an indicator variable representing whether the process is out-of-control at time k defined as follows:

$$A_k = \begin{cases} 1, & \textit{if } X_t \text{ is classified as out-of-control,} \\ 0, & \text{otherwise.} \end{cases} \quad (9)$$

The windowing process begins by identifying the first anomaly, X_{k_1} for $k_1 = min\{k|\ A_k = 1\}$, which is the smallest index k where the process is detected as out-of-control. For each subsequent point $k > k_1$, a decision-making procedure is applied based on whether k lies within or beyond the window $[k_1, k_1 + W]$. When k is within the window, the point X_k is deemed non-anomalous. However, if k is beyond the window, the next anomaly is identified as X_{k_2} where $k_2 = min\{k|\ A_k = 1,\ k\rangle k_1 + W\}$ and a new window $[k_2, k_2 + W]$ is defined, updating the reference point to k_2.

This process iterates continuously, applying the same logic to each subsequent out-of-control point where redundant points within the current window are discarded, and the window is updated when a new out-of-control point is identified beyond its bounds. This ensures that only the first out-of-control point in each window is retained, effectively filtering out non-anomalous points. The final output is a refined set of out-of-control points, where only the most significant anomalies are preserved and redundant points are eliminated.

2.4 | Design and Implementation of the WMD-EWMA Control Chart

The WMD-EWMA operates in three primary phases: retrospective, prospective, and windowed out-of-control mitigation phases. Many studies use covariate drift to describe changes in input variable distributions over time, affecting control limits from the retrospective phase. A covariate drift indicates a transition from stationary to non-stationary data, suggesting process or environmental changes. However, this paper focusses on distinguishing between in-control and out-of-control states. The WMD-EWMA control chart detects deviations from control limits set in the retrospective phase. If new data points fall outside these limits, it indicates an out-of-control condition rather than a covariate drift. Thus, the emphasis here is on managing false positives and

ALGORITHM 1 | Retrospective phase.

1. Initialise $Z_0 = \frac{1}{t_n}\sum_{t=1}^{t_n} X_t$, $E_0 = 0$ & specify a range of values for λ, where $0 < \lambda \leq 1$.
2. Compute the EWMA statistics, Z_t for all $t = 1, 2, \ldots, t_n$.
3. Calculate the one-step-ahead prediction errors, E_t for all $t = 1, 2, \ldots, t_n$.
4. Compute the time-independent variance estimate of the prediction error, $\hat{\sigma}_E^2 = \left(\frac{1}{t_n}\sum_{t=1}^{t_n} E_t^2\right)^2$.
5. Advance to prospective phase when $\hat{\sigma}_E^2$ is minimised for a specific λ.

ALGORITHM 2 | Prospective phase.

1. Initialise α which is chosen arbitrary (say, $\alpha = 0.01$ as recommended by Montgomery and Mastrangelo (1991)), $\hat{\sigma}_{E_0} \approx 0$, $ARL_0 = 350$ and include all retrospective phase results.
2. Set L_{WMD} to some specific value to achieve the initialised ARL_0.
3. For all $t = t_{n+1}, t_{n+2}, \ldots, T$:
   a. Compute the EWMA statistic, Z_t.
   b. Compute the one-step-ahead prediction error, E_t
   c. Compute the time-dependent variance estimate of the prediction error, $\hat{\sigma}_{E_t}^2 = \alpha E_t^2 + (1-\alpha)\hat{\sigma}_{E_{t-1}}^2$.
   d. Compute the control limits $LCL_{WMD_t} / UCL_{WMD_t} = Z_{t-1} \pm L_{WMD}\hat{\sigma}_{E_{t-1}}$.
   e. When $Z_t < LCL_{WMD_t}$ or $Z_t > UCL_{WMD_t}$ then go to the windowed out-of-control mitigation phase.

identifying true process changes versus isolated deviations. The three phases are detailed as follows:

2.4.1 | Retrospective Phase

In this phase, the algorithm calculates baseline parameters from historical data, assuming these data represent a stationary state of an in-control process, specifically, $\{X_t\}$ for $t = 1, 2, \ldots, t_n$, where t_n is a relevant time period. This phase involves steps summarised in Algorithm 1.

2.4.2 | Prospective Phase

In this phase, the algorithm monitors new incoming data representing a non-stationary state of an out-of-control process, specifically, $\{X_t\}$ for $t = t_n + 1, t_n + 2, \ldots, T$, where T is the final time point. This phase includes the steps summarised in Algorithm 2.

ALGORITHM 3 | Windowed out-of-control mitigation phase.

1. Set the window length W (say, $W = 10$) and classify the first anomaly as X_{k_1} where $k_1 = min\{k|\ A_k = 1\}$
2. For each subsequent $k > k_1$,
   a. If $k \in [k_1, k_1 + W]$, then X_k are non-anomalous.
   b. If $k > k_1 + W$ then set X_{k_2} to be the second anomaly for $k_2 = \min\{k|\ A_k = 1,\ k > k_1 + W\}$ whilst updating the window $[k_2, k_2 + W]$.
   c. The process continues iteratively until all out-of-control points have been processed.

2.4.3 | Windowed Out-of-Control Mitigation Phase

In this phase, the algorithm employs a window-based filtering strategy to reduce false positives, ensuring that only the first detected out-of-control observation within each window is retained as an anomaly. The steps of this phase are outlined in Algorithm 3.

2.5 | Performance Metrics

The following metrics are chosen for their relevance to this study, with the goal of minimising false positives and thereby reducing the *ARL* for out-of-control processes. Note that the following terminology is used interchangeably: a mean drift, drift, true positive and anomaly. Whereas, the following metrics are used to evaluate the control charts:

- True positive (TP): Correctly detecting a mean drift when one actually exists.
- False positive (FP): Incorrectly detecting a mean drift when none exists (Type-I error).
- False negative (FN): Failing to detect a mean drift when one exists (Type-II error).
- True negative (TN): Correctly identifying that no mean drift exists when there is none.
- Accuracy (%): Percentage of correctly identified observations, denoted as

$$Accuray\ \ (\%) = \frac{TP + TN}{TP + FP + TN + FN} \times 100 \qquad (10)$$

- The attained in-control *ARL* (*ICARL*): Average number of rational points plotted on the chart before the first out-of-control signal when there is no drift in the process.
- The out-of-control $ARL(ARL_1)$: Average number of rational points plotted on the chart before the first out-of-control signal when there is a drift $\delta(\delta \neq 0)$.

The run-length is computed using the following expression:

$$RL = min\{t|X_t \notin [LCL, UCL]\}, \qquad (11)$$

where X_t represents the charting statistic and $t \in \mathbb{N}\backslash\{0\}$.

To investigate the overall performance of a chart, it is often recommended to use the expected *ARL* (*EARL*). In this paper, the performances of the proposed charts are evaluated in terms of the *EARL* and expected standard deviation of the run length (*ESDRL*) profiles. Thus, the *EARL* and *ESDRL* values are given by

$$EARL = \frac{1}{\Delta}\sum_{\delta=\delta_{\min}}^{\delta_{\max}} ARL(\delta),$$

and

$$SDRL = \frac{1}{\Delta}\sum_{\delta=\delta_{\min}}^{\delta_{\max}} SDRL(\delta), \tag{12}$$

respectively, where $ARL(\delta)$ and $SDRL(\delta)$ represent the OOC *ARL* and *SDRL* (ARL_1 and $SDRL_1$) for a specific drift (δ), the symbol Δ denotes the number of increments between the lower and upper bound shifts (i.e., δ_{min} and δ_{max}).

3 | Performance Analysis

In this section, the performance of the WMD-EWMA chart from small to large mean drifts is compared with that of the MD-EWMA, traditional EWMA and other competing control charts in terms of the *ARL* profile, standard deviation of the run length (*SDRL*) and percentage accuracy as described in Section 2.5.

3.1 | Performance Comparison

In this section, specific performances (*ARL* and *SDRL* profiles) and overall performances (*EARL* and *ESDRL* profiles) of the proposed MD- and WMD-EWMA charts are compared to the performances of the existing Shewhart, EWMA and CUSUM charts for individual observations with a nominal in-control *ARL* (ARL_0) of 350. In Tables 1 and 2, the CUSUM chart's reference value k_c is set to 0.5 (i.e., $k = 0.5$) and the smoothing parameters of the MD- and WMD-EWMA charts are both set to be equal to $1-\theta$ (i.e., $\lambda = 1-\theta$), as explained in Section 2.2. In Tables 1 and 2, the *SDRL* and *ESDRL* profiles are displayed in parentheses. The window length of the WMD-EWMA chart is equal to 150 (i.e., $W = 150$). The computation of the performance is done using 10000 simulations with data generated from the standard normal distribution (i.e., $N(0,1)$) and $\theta \in \{0.1, 0.25, 0.5, 0.6, 0.75, 0.9\}$. The window length is selected as a practical benchmark that accounts for sporadic drift occurrence while mitigating false positives from post-drift variance. The control limit constants of the Shewhart, CUSUM, EWMA, MD-EWMA and WMD-EWMA charts were found to be equal to 3.054, 4.846, 2.954, 2.731 and 2.635, respectively so that they yield *ICARL* values equal or much closer to the ARL_0 of 350. In terms of the *ARL* profile, the results show that as θ increases, the sensitivity of the proposed MD- and WMD-EWMA charts increases as well. The WMD-EWMA chart outperforms the competing charts followed by the MD-EWMA chart regardless of the size of the drift. It can also be observed that the proposed charts are efficient for monitoring small to large mean drifts. The performances of the standard CUSUM and EWMA charts are almost similar and they both outperform the standard Shewhart chart for small to moderate drifts. However, for large drifts, the Shewhart chart performs slightly better than the CUSUM and EWMA charts. In terms of the *SDRL* profile, the results displayed in Tables 1 and 2 reveal that for larger values of λ, which correspond to smaller values of θ, the proposed charts are likely to give more false alarms. However, it is noteworthy that the false alarm rates from the proposed charts remain lower in comparison to those generated by the existing Shewhart, CUSUM, and EWMA charts. As θ increases, the charts under consideration are likely to give less false alarms. In terms of the *EARL* and *ESDRL* profiles, Tables 1 and 2 show that the WMD-EWMA chart is superior over the competing charts followed by the MD-EWMA chart regardless of the level of θ.

To clearly show the difference between the competing charts, their performances are compared in terms of the comparison ratio (denoted as C_r). The C_r represents the ratio of the competing chart to the benchmark chart. In this paper, the benchmark chart is the WMD-EWMA chart

The C_r is then defined by

$$C_r = \frac{ARL_c(\delta)}{ARL^*(\delta)}, \tag{13}$$

where $ARL_c(\delta)$ is the *ARL* value of the competing chart for a specific mean drift and $ARL^*(\delta)$ is the *ARL* value of the benchmark chart for the same mean drift.

The C_r value is interpreted as follows:

- when $C_r > 1$, the WMD-EWMA chart performs better than the competing chart.
- when $C_r < 1$, the competing chart outperforms the WMD-EWMA chart.
- when $C_r = 1$, the competing and benchmark charts perform similarly.

Tables 3 and 4 show that confirm that the WMD-EWMA chart outperforms all competing charts as its C_r values consistently equal 1, whereas that of the competing charts are greater than 1.

3.2 | Accuracy of the Proposed Charts

In this section, the accuracy of the proposed chart in identifying mean drifts in the process is investigated in terms of the accuracy metric. Note that Figure 1 displays the accuracy ratio of the MD- and WMD EWMA charts in detecting drifts in the process parameter. Figure 1 shows that the detection accuracy of the MD-EWMA chart increases as the drift size increases (see, Figure 1(a)). It can also be observed that the WMD-EWMA chart is more accurate than the MD-EWMA chart. For instance, for a drift of 0.25 standard deviation, the WMD-EWMA chart is 1.6% and 43.5% more accurate than the MD-EWMA chart when $W = 10$ and 200, respectively. For a moderate drift of 1.5 standard deviation, the WMD-EWMA chart is 5% and 21% more accurate than the MD-EWMA chart when $W = 10$ and 200, respectively (see, Figure 1(a,b)). From Figure 1(b), it can be seen that the detection accuracy of the WMD-EWMA chart increases with the increase in the window length. For a fixed window length, the

TABLE 1 | Comparison of specific and overall performances of the MD- and WMD-EWMA charts with that of the standard Shewhart, CUSUM and EWMA charts for individual observations when $ARL_0 = 350$ and $\theta \in \{0.1, 0.25, 0.5\}$.

$\theta = 1 - \lambda$	Drift	Shewhart	CUSUM	EWMA	MD-EWMA	WMD-EWMA
0.1	0.00	350.6 (346.5)	351.4 (356.6)	350.8 (351.9)	351.1 (345.5)	349.5 (341.8)
	0.25	244.3 (242.7)	89.3 (82.1)	92.1 (81.7)	81.6 (70.6)	69.5 (61.2)
	0.50	138.5 (129.1)	30.1 (24.5)	31.2 (24.8)	23.3 (15.8)	18.7 (12.4)
	0.75	91.3 (87.4)	19.4 (16.2)	20.6 (16.5)	17.6 (11.2)	15.4 (8.1)
	1.00	34.2 (31.3)	8.8 (7.9)	9.1 (8.0)	8.2 (6.9)	6.4 (5.7)
	1.25	22.4 (19.5)	7.0 (6.9)	6.9 (6.6)	5.9 (6.0)	5.1 (4.8)
	1.50	13.4 (10.1)	6.2 (5.4)	6.0 (5.3)	5.2 (4.4)	4.6 (3.9)
	1.75	8.3 (6.7)	5.4 (4.8)	5.3 (4.7)	4.2 (3.5)	3.7 (3.0)
	2.00	4.7 (3.0)	4.1 (3.2)	4.0 (3.0)	3.8 (2.7)	3.3 (2.3)
	2.25	3.2 (2.1)	3.5 (2.2)	3.4 (2.2)	2.9 (1.8)	2.5 (1.7)
	2.50	2.5 (1.6)	3.1 (1.6)	3.0 (1.6)	2.6 (1.3)	2.1 (1.2)
	2.75	2.3 (1.4)	2.8 (1.5)	2.7 (1.4)	1.9 (1.0)	1.6 (0.9)
	3.00	2.0 (1.2)	2.4 (1.2)	2.3 (1.1)	1.6 (0.9)	1.4(0.7)
EARL (*ESDRL*)		47.3 (44.7)	15.2 (13.1)	15.6 (13.1)	13.2 (10.5)	11.2 (8.8)
0.25	0.25	194.4 (189.2)	50.2 (43.3)	52.4 (44.6)	42.2 (36.3)	34.4 (28.1)
	0.50	98.2 (91.3)	20.5 (16.2)	21.1 (16.9)	17.8 (13.4)	14.8 (10.3)
	0.75	39.5 (33.4)	15.1 (11.5)	15.7 (11.7)	12.4 (6.1)	10.8 (4.8)
	1.00	26.3 (22.2)	7.5 (4.1)	7.7 (4.2)	6.9 (3.2)	5.8 (2.9)
	1.25	15.1 (10.4)	6.6 (3.6)	6.5 (3.6)	5.4 (2.9)	4.6 (2.2)
	1.50	10.4 (7.9)	5.3 (3.1)	4.9 (3.0)	4.1 (2.5)	3.9 (1.9)
	1.75	6.8 (4.8)	4.9 (2.8)	4.8 (2.7)	3.8 (2.0)	3.1 (1.6)
	2.00	4.2 (2.0)	4.0 (2.5)	4.0 (2.5)	3.1 (1.9)	2.8 (1.4)
	2.25	2.9 (1.6)	3.1 (2.0)	2.9 (1.9)	2.4 (1.7)	2.2 (1.3)
	2.50	2.2 (1.3)	2.6 (1.8)	2.5 (1.8)	1.9 (1.5)	1.6 (1.1)
	2.75	1.9 (1.1)	2.5 (1.3)	2.4 (1.2)	1.6 (1.0)	1.4 (0.8)
	3.00	1.7 (0.9)	2.1 (1.1)	2.0 (1.0)	1.5 (0.8)	1.3 (0.6)
EARL (*ESDRL*)		33.6 (30.5)	10.4 (7.8)	10.6 (7.9)	8.6 (6.1)	7.2 (4.8)
0.5	0.25	89.6 (80.8)	25.0 (21.3)	24.6 (21.0)	21.4 (16.5)	19.5 (14.2)
	0.50	31.2 (23.4)	11.1 (5.1)	10.9 (4.8)	10.2 (4.2)	8.5 (4.0)
	0.75	12.9 (6.8)	8.5 (4.7)	8.3 (4.5)	6.7 (3.9)	5.6 (3.6)
	1.00	7.0 (4.0)	6.0 (3.3)	5.8 (3.4)	4.1 (3.3)	3.2 (3.2)
	1.25	3.6 (2.2)	4.7 (2.6)	4.5 (2.7)	3.7 (2.4)	3.1 (2.2)
	1.50	2.7 (1.9)	3.9 (2.2)	3.9 (2.2)	3.0 (1.9)	2.4 (1.8)
	1.75	2.4 (1.6)	3.2 (2.0)	3.1 (1.9)	2.5 (1.7)	2.1 (1.6)
	2.00	2.3 (1.5)	2.9 (1.8)	2.9 (1.8)	2.1 (1.4)	1.7 (1.3)
	2.25	2.1 (1.3)	2.6 (1.6)	2.5 (1.6)	1.9 (1.3)	1.6 (1.1)
	2.50	2.0 (1.2)	2.4 (1.4)	2.4 (1.3)	1.7 (1.1)	1.5 (1.0)
	2.75	1.8 (1.0)	2.1 (1.2)	2.2 (1.2)	1.5 (0.9)	1.3 (0.9)
	3.00	1.6 (0.8)	2.0 (1.1)	2.0 (1.0)	1.4 (0.9)	1.1 (0.8)
EARL (*ESDRL*)		8.6 (6.4)	5.0 (2.9)	4.9 (2.9)	3.9 (2.4)	3.3 (2.2)

TABLE 2 | Comparison of specific and overall performances of the MD- and WMD-EWMA charts with that of the standard Shewhart, CUSUM and EWMA charts for individual observations when $ARL_0 = 350$ and $\theta \in \{0.6, 0.75, 0.9\}$.

$\theta = 1 - \lambda$	Drift	Shewhart	CUSUM	EWMA	MD-EWMA	WMD-EWMA
0.6	0.25	79.3 (70.4)	21.0 (15.7)	20.6 (15.3)	18.1 (13.9)	16.5 (18.1)
	0.50	26.4 (16.9)	9.2 (7.9)	9.1 (7.8)	8.0 (6.9)	7.4 (6.4)
	0.75	10.1 (8.5)	5.8 (4.8)	5.7 (4.9)	5.0 (3.8)	4.1 (3.3)
	1.00	6.0 (6.2)	4.4 (4.0)	4.2 (3.9)	3.4 (2.5)	2.9 (2.0)
	1.25	4.7 (3.4)	3.9 (2.9)	3.6 (2.7)	2.9 (1.3)	2.5 (1.7)
	1.50	3.2 (2.3)	3.1 (1.6)	3.0 (1.5)	2.6 (1.2)	2.2 (1.0)
	1.75	2.8 (1.5)	2.9 (1.4)	2.8 (1.3)	2.3 (1.1)	1.9 (0.9)
	2.00	2.2 (1.2)	2.7 (1.3)	2.7 (1.3)	2.0 (1.0)	1.7 (0.8)
	2.25	2.1 (1.1)	2.5 (1.1)	2.5 (1.2)	1.7 (0.9)	1.5 (0.8)
	2.50	1.7 (1.0)	2.4 (1.0)	2.3(0.9)	1.6 (0.8)	1.3 (0.7)
	2.75	1.6 (0.9)	2.1 (0.9)	2.2 (0.8)	1.3(0.7)	1.1 (0.6)
	3.00	1.5 (0.9)	2.0 (0.8)	2.0 (0.8)	1.1 (0.7)	1.0 (0.5)
EARL (*ESDRL*)		11.8 (9.5)	5.2 (3.6)	5.1 (3.5)	4.2 (2.9)	3.7 (3.1)
(0.6)0.75	0.25	41.5 (33.5)	15.1 (11.0)	14.4 (10.8)	11.2 (5.6)	9.7 (5.1)
	0.50	16.2 (12.9)	8.3 (4.1)	8.2 (4.0)	6.1 (3.1)	5.6 (2.9)
	0.75	6.2 (3.6)	5.2 (2.9)	5.3 (2.8)	4.5 (2.5)	3.9 (2.2)
	1.00	4.6 (2.9)	3.8 (2.4)	3.9 (2.4)	3.3 (2.2)	3.2 (1.8)
	1.25	4.1 (2.5)	3.4 (2.0)	3.6 (2.1)	2.9 (1.9)	2.6 (1.5)
	1.50	3.2 (1.9)	3.1 (1.8)	3.1 (1.9)	2.5 (1.6)	2.1 (1.3)
	1.75	2.6 (1.7)	2.9 (1.7)	3.0 (1.7)	2.2 (1.4)	1.8 (1.2)
	2.00	2.1 (1.3)	2.5 (1.4)	2.5 (1.3)	1.9 (1.2)	1.6 (1.0)
	2.25	1.9 (1.1)	2.3 (1.2)	2.2 (1.1)	1.6 (1.0)	1.4 (0.8)
	2.50	1.7 (1.0)	2.1 (1.2)	2.1 (1.1)	1.5 (0.8)	1.2 (0.7)
	2.75	1.4 (0.9)	2.0 (1.0)	2.0 (0.9)	1.2 (0.8)	1.1 (0.6)
	3.00	1.5 (0.8)	2.0 (0.9)	2.0(0.8)	1.0 (0.6)	1.0 (0.5)
EARL (*ESDRL*)		7.3 (5.3)	4.4 (2.6)	4.4 (2.6)	3.3 (1.9)	2.9 (1.6)
0.9	0.25	12.4 (6.3)	11.3 (5.5)	11.1 (5.4)	9.8 (4.9)	7.9 (4.2)
	0.50	7.1 (4.0)	6.7 (3.8)	6.5 (3.7)	5.9 (3.2)	4.8 (2.9)
	0.75	5.6 (3.2)	5.0 (3.0)	4.9 (3.0)	4.4 (2.6)	3.9 (2.3)
	1.00	3.6 (2.8)	3.6 (2.7)	3.5 (2.6)	3.3 (2.3)	2.7 (1.9)
	1.25	3.0 (2.6)	3.3 (2.4)	3.4 (2.3)	3.1 (2.0)	2.4 (1.6)
	1.50	2.8 (1.9)	2.9 (1.7)	3.0 (1.7)	2.5 (1.5)	2.2 (1.4)
	1.75	2.5 (1.7)	2.7 (1.6)	2.8 (1.5)	1.9 (1.2)	1.7 (1.1)
	2.00	1.9 (1.5)	2.4 (1.5)	2.4 (1.4)	1.6 (1.0)	1.4 (1.0)
	2.25	1.7 (1.3)	2.2 (1.4)	2.1(1.4)	1.4 (0.8)	1.3 (0.8)
	2.50	1.5 (1.2)	2.0 (1.2)	2.0 (1.2)	1.3 (0.7)	1.1 (0.7)
	2.75	1.3 (1.0)	2.0 (1.1)	2.0 (1.0)	1.0 (0.6)	1.0 (0.6)
	3.00	1.2 (0.7)	2.0 (0.8)	2.0 (0.7)	1.0 (0.6)	1.0 (0.4)
EARL (*ESDRL*)		3.7 (2.4)	3.8 (2.2)	3.8 (2.2)	3.1 (1.8)	2.6 (1.6)

TABLE 3 | The C_r value of the MD- and WMD-EWMA charts with that of the standard Shewhart, CUSUM and EWMA charts for individual observations when $ARL_0 = 350$ and $\theta \in \{0.1, 0.25, 0.5\}$.

$\Theta = 1 - \lambda$	Drift	Shewhart	CUSUM	EWMA	MD-EWMA	WMD-EWMA
0.1	0.00	1.0	1.0	1.0	1.0	1.0
	0.25	3.5	1.3	1.3	1.2	1.0
	0.50	7.4	1.6	1.7	1.2	1.0
	0.75	5.9	1.3	1.3	1.1	1.0
	1.00	5.3	1.4	1.4	1.3	1.0
	1.25	4.4	1.4	1.4	1.2	1.0
	1.50	2.9	1.3	1.3	1.1	1.0
	1.75	2.2	1.5	1.4	1.1	1.0
	2.00	1.4	1.2	1.2	1.2	1.0
	2.25	1.3	1.4	1.4	1.2	1.0
	2.50	1.2	1.5	1.4	1.2	1.0
	2.75	1.4	1.8	1.7	1.2	1.0
	3.00	1.4	1.7	1.6	1.1	1.0
0.25	0.25	5.7	1.5	1.5	1.2	1.0
	0.50	6.6	1.4	1.4	1.2	1.0
	0.75	3.7	1.4	1.5	1.1	1.0
	1.00	4.5	1.3	1.3	1.2	1.0
	1.25	3.3	1.4	1.4	1.2	1.0
	1.50	2.7	1.4	1.3	1.1	1.0
	1.75	2.2	1.6	1.5	1.2	1.0
	2.00	1.5	1.4	1.4	1.1	1.0
	2.25	1.3	1.4	1.3	1.1	1.0
	2.50	1.4	1.6	1.6	1.2	1.0
	2.75	1.4	1.8	1.7	1.1	1.0
	3.00	1.3	1.6	1.5	1.2	1.0
0.5	0.25	4.6	1.3	1.3	1.1	1.0
	0.50	3.7	1.3	1.3	1.2	1.0
	0.75	2.3	1.5	1.5	1.2	1.0
	1.00	2.2	1.9	1.8	1.3	1.0
	1.25	1.2	1.5	1.5	1.2	1.0
	1.50	1.1	1.6	1.6	1.3	1.0
	1.75	1.1	1.5	1.5	1.2	1.0
	2.00	1.4	1.7	1.7	1.2	1.0
	2.25	1.3	1.6	1.6	1.2	1.0
	2.50	1.3	1.6	1.6	1.1	1.0
	2.75	1.4	1.6	1.7	1.2	1.0
	3.00	1.5	1.8	1.8	1.3	1.0

detection accuracy of the WMD-EWMA chart increases as the mean drift increases. In other words, the smaller the drift, the more likely the noise will cause interference in the data. The larger the drift, the more accurate the proposed charts are in detecting drifts. As the drift increases, the detection accuracy ratio tends to 1.

3.3 | Illustrative Discussion of the Implementation, Design and Performance of the Proposed Charts

Results in this section are rounded to three decimal places, where relevant, for demonstrative purposes. The goal is to accurately

TABLE 4 | The C_r value of the MD- and WMD-EWMA charts with that of the standard Shewhart, CUSUM and EWMA charts for individual observations when $ARL_0 = 350$ and $\theta \in \{0.6, 0.75, 0.9\}$.

$\Theta = 1 - \lambda$	Drift	Shewhart	CUSUM	EWMA	MD-EWMA	WMD-EWMA
0.6	0.25	4.8	1.3	1.2	1.1	1.0
	0.50	3.6	1.2	1.2	1.1	1.0
	0.75	2.5	1.4	1.4	1.2	1.0
	1.00	2.1	1.5	1.4	1.2	1.0
	1.25	1.9	1.6	1.4	1.2	1.0
	1.50	1.5	1.4	1.4	1.2	1.0
	1.75	1.5	1.5	1.5	1.2	1.0
	2.00	1.3	1.6	1.6	1.2	1.0
	2.25	1.4	1.7	1.7	1.1	1.0
	2.50	1.3	1.8	1.8	1.2	1.0
	2.75	1.5	1.9	2.0	1.2	1.0
	3.00	1.5	2.0	2.0	1.1	1.0
0.75	0.25	3.2	1.4	1.4	1.1	1.0
	0.50	4.3	1.6	1.5	1.2	1.0
	0.75	2.9	1.5	1.5	1.1	1.0
	1.00	1.6	1.3	1.4	1.2	1.0
	1.25	1.4	1.2	1.2	1.0	1.0
	1.50	1.6	1.3	1.4	1.1	1.0
	1.75	1.5	1.5	1.5	1.2	1.0
	2.00	1.4	1.6	1.7	1.2	1.0
	2.25	1.3	1.6	1.6	1.2	1.0
	2.50	1.4	1.6	1.6	1.1	1.0
	2.75	1.4	1.8	1.8	1.3	1.0
	3.00	1.3	1.8	1.8	1.1	1.0
0.9	0.25	1.5	2.0	2.0	1.0	1.0
	0.50	2.5	1.5	1.5	1.1	1.0
	0.75	1.6	1.4	1.4	1.2	1.0
	1.00	1.5	1.4	1.4	1.2	1.0
	1.25	1.4	1.3	1.3	1.1	1.0
	1.50	1.3	1.3	1.3	1.2	1.0
	1.75	1.3	1.4	1.4	1.3	1.0
	2.00	1.3	1.3	1.4	1.1	1.0
	2.25	1.5	1.6	1.6	1.1	1.0
	2.50	1.4	1.7	1.7	1.1	1.0
	2.75	1.3	1.7	1.6	1.1	1.0
	3.00	1.4	1.8	1.8	1.2	1.0

detect the first significant mean drifts in autocorrelated data (acting as the anomaly occurrence) while minimising false positives. Four datasets are under consideration: two synthetic datasets, which are used for demonstrative purposes to validate the approach's applicability to real data and two real-world datasets, one containing significant mean drifts and the other characterised by spiky data. All datasets of the WMD-EWMA control charts have a window length of $W = 10$, and the rationale for this choice is provided for each dataset.

The control charts displayed in this section have the same layout. The retrospective phase is represented by observations without the pink shading, while the prospective phase is indicated by observations with pink shading. This pink shading represents the

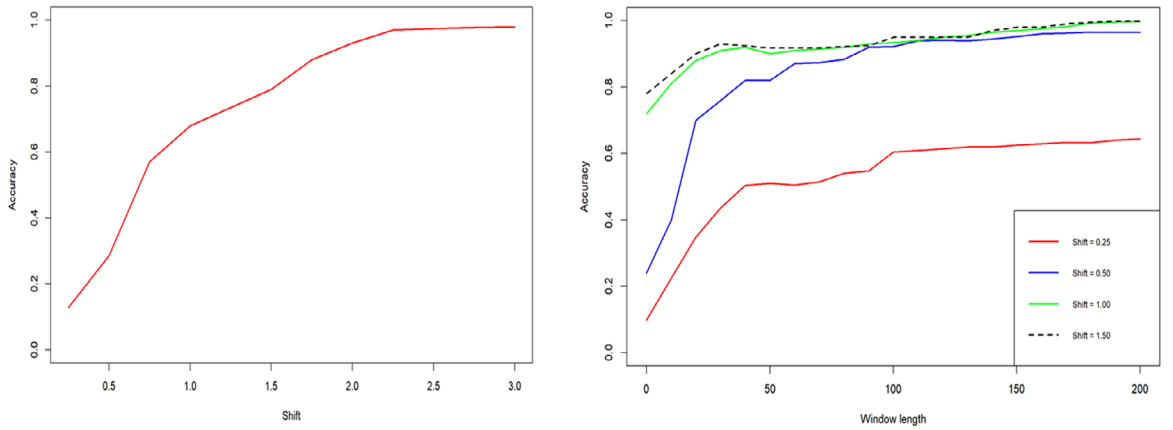

(a) MD-EWMA chart (b) WMD-EWMA chart

FIGURE 1 | Accuracy of the proposed chart for different drift sizes.

control limits of the chart under consideration. The pink line illustrates the observed behaviour over time and the purple dots mark the detected out-of-control points. In this section, a window length of $W = 10$ is employed, as mean drifts are anticipated to occur occasionally, while modest variation is expected after a drift. A window length of $W = 150$, used in Section 3.1, illustrates that anomalies occur more sporadically, while also allowing better management of uncontrolled variance.

Additionally, we investigate the performance in terms of the run-length distribution of the proposed chart. all in-control run-length (RL_0) distributions along with their characteristics are presented in Appendix B. These RL_0 distributions highlight the variability and potential for long tails, which can significantly affect control chart performance. The visualisation of such distributions enables a deeper analysis through percentile metrics, which is beyond this paper's interest, offering insights into how the control chart manages variations in false alarm rates, especially in scenarios with extended or atypical drifts in the data.

3.3.1 | Single Mean Drift Dataset (D_1)

This synthetic dataset, referred to as D_1, consists of 100 observations with a sudden drift at time point 51 where the distribution changes from $N(1,1)$ to $N(6,1)$. No assumptions of independence are made for the observations, so the data may exhibit autocorrelation. This drift simulates a non-stationary process. The RL_0 distribution is showcased in Appendix B (see Figure B1), which has a control limit multiplier $L_{WMD} = 3.015$ that achieves an $ARL_0 = 350$.

Figure 2 presents the control charts for the WMD-EWMA and MD-EWMA methods applied to D_1. Both charts capture the anomaly, but the MD-EWMA chart detected more out-of-control observations. Specifically, the evaluation metrics presented in Table 5 shows that the MD-EWMA method produces three false positives, indicating spurious anomalies. In contrast, the WMD-EWMA chart employs a windowed out-of-control mitigation strategy, using a window length of $W = 10$ to effectively reduce false positives.

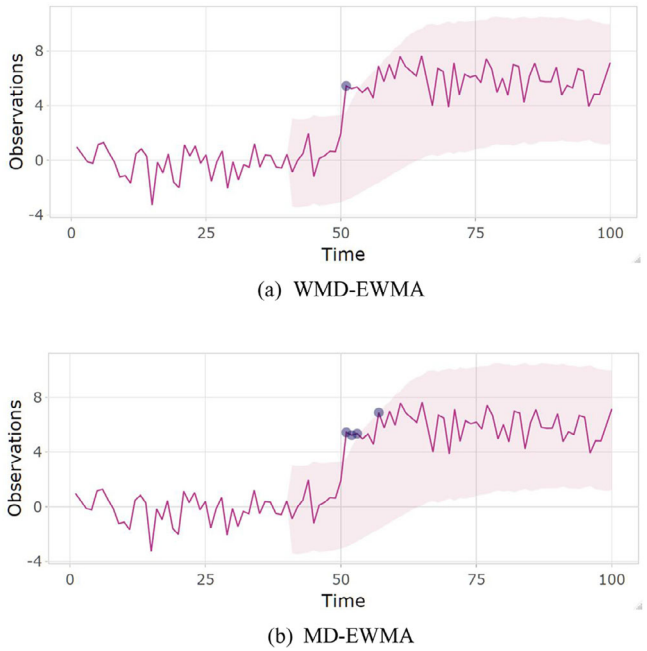

(a) WMD-EWMA

(b) MD-EWMA

FIGURE 2 | WMD-EWMA and MD-EWMA control charts for dataset D_1.

The window length W is a critical parameter in the WMD-EWMA control chart, as it directly influences the trade-off between anomaly detection sensitivity and false positive rates. A window that is too short (e.g., $W = 2$) risks flagging post-drift process variability as additional shifts. Conversely, an excessively long window (e.g., $W = 50$) would be overly conservative, potentially missing drifts that occur more frequently as the process continues. The choice of $W = 10$ provides an optimal compromise: it allows sufficient time after a detected drift to avoid flagging transient variance fluctuations as new anomalies, while remaining responsive enough to detect subsequent drifts occurring at realistic intervals.

The accuracy rates, as presented in Table 5, further demonstrate the superior performance of the WMD-EWMA method, which achieved 100% accuracy compared to the 97% accuracy of the MD-

TABLE 5 | Comparing of WMD-EWMA and MD-EWMA control charts for dataset D_1.

Evaluation metrics	WMD-EWMA	MD-EWMA
TP	1	1
FP	0	3
FN	0	0
TN	99	96
Accuracy (%)	100	97

EWMA chart. This improvement underscores the effectiveness of the windowed enhancement in the WMD-EWMA approach, making it more reliable for detecting significant drifts without being misled by transient noise. Thus, for dataset D_1, the WMD-EWMA chart exhibits improved accuracy and better control over false alarm rates. Its ability to detect the significant drift while avoiding false positives demonstrates its effectiveness in handling non-stationary processes with sudden mean drifts.

3.3.2 | Multiple Mean Drifts (D_2)

The generated dataset D_2 consists of 500 observations, which may exhibit autocorrelation and are not limited to an assumption of independence. Modelling a non-stationary time series that is described by

$$x_t = 0.6\, x_{t-1} - 0.5\, x_{t-2} + \varepsilon_t, \tag{14}$$

where $\varepsilon_t \sim N(\mu_D, 0.5)$ and $x_1 = x_2 = 0$.

The mean, μ_D, undergoes drifts at every hundredth observation, starting from 1 and increasing by D units with each drift, as defined by

$$\mu_D = \begin{cases} 0, & when\ D = 1 \\ \mu_{D-1} + D, & when\ D = 2, 3, 4, 5 \end{cases} \tag{15}$$

Similar to the analysis of D_1, the RL_0 distribution for D_2 is presented in Appendix B (see Figure B2) with an $ARL_0 = 350$ when $L_{WMD} = 2.98576$, showcasing the variability and potential long tails that may influence control chart performance. For the WMD-EWMA control chart, an optimal window length of W =10 is selected for D_2, applying the same rationale as discussed for D_1. This choice balances responsiveness to reasonable mean drifts while accounting for the autocorrelation structure that may amplify short-term fluctuations immediately following drift detection.

Figure 3 compares the WMD-EWMA and MD-EWMA control charts for the D_2 dataset, illustrating how both methods successfully identify all true positives corresponding to the intentional mean drifts. The WMD-EWMA chart displays a cleaner and more precise detector of drifts, while the MD-EWMA chart shows additional fluctuations corresponding to its false positives.

Table 6 showcases that the WMD-EWMA chart demonstrated flawless performance, with no false positives, false negatives and

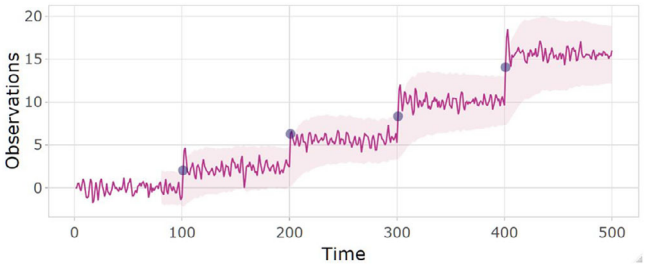

(a) WMD-EWMA control chart

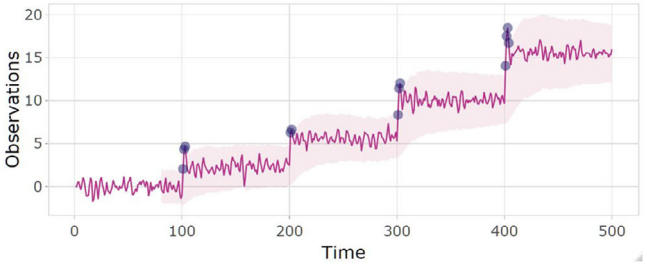

(b) MD-EWMA control chart

FIGURE 3 | WMD-EWMA and MD-EWMA control charts for dataset D_2.

TABLE 6 | Comparison of WMD-EWMA and MD-EWMA control charts for dataset D_2.

Evaluation metrics	WMD-EWMA	MD-EWMA
TP	4	4
FP	0	8
FN	0	0
TN	496	488
Accuracy (%)	100	98.4

correctly identifying all true negatives, resulting in a perfect accuracy rate of 100%. This underscores its effectiveness in precisely detecting all mean drifts in D_2 while minimising the risk of false alarms. In contrast, the MD-EWMA chart, although it detected all true positives without any false negatives, generated eight false positives, leading to a slightly lower accuracy of 98.4%.

3.3.3 | Real World Data (D_3)

The MD-EWMA and WMD-EWMA control charts were tested thus far under controlled environments. This gave an indication that applying both control charts to uncontrolled environments that have a significant mean drift in the process could be highly beneficial.

Dataset D_3 consists of real-time petal lengths from the well-known cross-sectional 'Fisher's Iris' dataset frequently used in statistical classification and machine learning demonstrations (see, Fisher [18]). As an intriguing approach, this dataset is treated as if observations were recorded over a uniform time span. The control limit multiplier was selected as $L_{WMD} = 3.03$ to achieve an

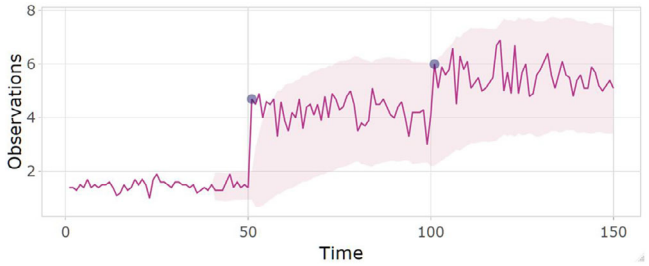

(a) WMD-EWMA control chart

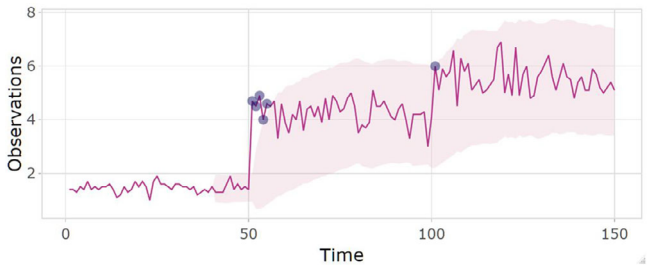

(b) MD-EWMA control chart

FIGURE 4 | WMD-EWMA and MD-EWMA control charts for dataset D_3.

TABLE 7 | Comparison of WMD-EWMA and MD-EWMA control charts for dataset D3.

Evaluation metrics	WMD-EWMA	MD-EWMA
TP	2	2
FP	0	4
FN	0	0
TN	148	144
Accuracy (%)	100	97.33

ARL_0 350. This RL_0 distribution, illustrated in Appendix B (see Figure B3), was determined by generating a gamma distribution representative of the actual data in the in-control state and estimating the distributional parameters accordingly, ensuring that the control limits are well-suited to the dataset. The window length of W =10 for the WMD-EWMA control chart is retained for this dataset, as the rationale established for the previous datasets remains applicable.

Figure 4 illustrates the WMD-EWMA and MD-EWMA control charts for dataset D_3. Both charts successfully detect the mean drifts in the Iris petal length data. However, the WMD-EWMA chart shows cleaner detections with fewer fluctuations, indicating its superior ability to filter out noise while capturing significant drifts. Although this cross-sectional dataset was treated as a time series for demonstration purposes, the three anomalies detected by the WMD-EWMA chart correspond to the transitions between the three Iris species (setosa, versicolor and virginica), demonstrating that the chart has the potential to capture meaningful patterns even in non-ideal scenarios.

Table 7 highlights the distinct performance differences between the WMD-EWMA and MD-EWMA methods. The WMD-EWMA chart achieved a flawless accuracy of 100%, outperforming the MD-EWMA chart, which reached 97.33%. This indicates that the WMD-EWMA method was able to accurately identify all drifts and no drift in the Iris petal length data without generating any false positives or negatives. Conversely, the MD-EWMA chart, while still highly accurate, was more prone to false alarms, producing four false positives.

For botanical research or quality control in Iris cultivation, the findings suggest that the WMD-EWMA control chart is effective for detecting genuine variations in petal lengths over time without generating false positives. This implies that the WMD-EWMA method can accurately identify meaningful changes in petal measurements, which might signal environmental stresses, genetic variations, or other factors of interest. Its high precision in detecting anomalies makes it a valuable tool for researchers and cultivators who need reliable data for monitoring flower morphology and ensuring the quality of their crops. Enhanced sensitivity of the WMD-EWMA chart could provide deeper insights into subtle trends and variations that might otherwise be missed, offering a more robust framework for analysing and interpreting botanical data.

3.3.4 | Case Study Dataset (D_4)

Promising results have been observed with the MD-EWMA and WMD-EWMA control charts when applied to real data with a known mean drift. As an innovative extension of this paper, both charts are now applied to spiky data, characterised by rapid fluctuations around the in-control mean without any significant drift, to evaluate their performance. This exploration aims to assess how these control charts handle data with irregular fluctuations and determine their robustness in detecting anomalies without the presence of a clear mean drift. By analysing their behaviour on such data, we can gain insights into the charts' sensitivity to noise and their ability to distinguish genuine anomalies from random variations, which is crucial for practical applications where mean drifts are not always the primary concern.

Dataset D_4 consists of real-time Amazon Web Services (AWS) server metrics collected from Amazon CloudWatch, with a specific focus on the CPU utilisation performance metric (see, Gontier et al. [19]). The control limit multiplier of $L_{WMD} = 2.9585$ was selected to achieve an $ARL_0 = 350$. This RL_0, illustrated in Appendix B (see Figure B4), was determined by generating a normal distribution representative of the actual data in the in-control state and estimating the distributional parameters accordingly, ensuring that the control limits are well-suited to the dataset. For methodological consistency, the WMD-EWMA control chart maintains a window length of W =10 for this dataset.

This case is especially intriguing as it highlights an in-control process mean of approximately 33.5. The behaviour of the control limits reflects their adjustment for autocorrelated data, meaning that not all spikes observed in the chart are necessarily anomalies. As illustrated in Figure 5, the process may have adjusted its mean in response to previous anomalies, suggesting that what initially appeared to be a problem is now stabilising—potentially due to factors such as the activation of computer cooling mechanisms.

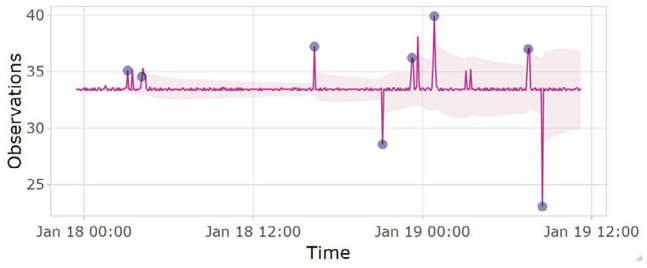

(a) WMD-EWMA control chart

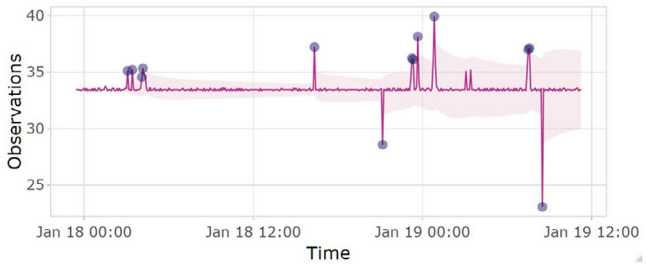

(b) MD-EWMA control chart

FIGURE 5 | WMD-EWMA and MD-EWMA control charts for dataset D_4.

This adaptive behaviour underscores the complexity of interpreting control charts, where apparent deviations may represent the system's natural response to transient disturbances rather than true anomalies.

Specifically, Figure 5 presents a comparison between the WMD-EWMA and MD-EWMA control charts when applied to dataset D4. Both charts successfully capture significant deviations in CPU utilisation. However, it is evident that the WMD-EWMA control chart has identified fewer out-of-control points compared to the MD-EWMA control chart. This reduction in detected anomalies is primarily attributed to the prespecified window length used in the WMD-EWMA method. In scenarios like this, where CPU utilisation exhibits frequent spikes, it may be necessary to adjust the window length based on expert knowledge and assumptions about how often such spikes are expected. Implementing run rules could also aid in the classification of these points, further refining the control process. The WMD-EWMA control chart is particularly advantageous in such situations because it is less prone to false positives while still effectively detecting substantial mean drifts and accounting for autocorrelated data. This reliability is crucial in environments where avoiding unnecessary alerts is as important as identifying genuine issues. In this case study, it is important to note that no evaluation metrics are directly presented to compare the performance of the WMD-EWMA and MD-EWMA methods. The discussion is grounded primarily on the visual inspection of the figures, allowing for an intuitive understanding of the charts' behaviour.

Thus, the WMD-EWMA control chart's performance on spiky data (used for experimental purposes) provides further insight into its adaptability. Spiky data, which does not involve large mean drifts, tests the chart's flexibility in different environmental settings. Although the WMD-EWMA chart did not capture all spikes (as it is not designed for this purpose), it successfully detected most of the significant mean drifts whilst considering the autocorrelation nature of the data, demonstrating that its performance is commendable even in non-ideal scenarios.

4 | Conclusion

This study demonstrates the effectiveness of incorporating a windowed out-of-control mitigation phase into the MD-EWMA control chart resulting in the WMD-EWMA control chart. The comparisons of the WMD-EWMA and MD-EWMA methods are primarily illustrative, showcasing how the windowing approach markedly enhances the detection of large mean drifts in autocorrelated data. Given that the WMD-EWMA control chart achieved a remarkable 100% accuracy in cases involving significant mean drifts, further comparisons with other control charts become unnecessary, as the WMD-EWMA has already proven to be the most effective method available.

While both the WMD-EWMA and MD-EWMA control charts naturally account for autocorrelation, only the WMD-EWMA chart has the added capability to reduce false positives in both controlled and uncontrolled settings—particularly when dealing with processes that exhibit large mean drifts. In scenarios where processes do not have a pronounced mean drift, such as in spiky data, both control charts remain effective due to the predictive ability and autocorrelation present in many modern-day problems. Traditional methods may fall short in such contexts, but the WMD-EWMA chart stands out as an enhanced approach for detecting large mean drifts in autocorrelated data, offering superior performance where it matters most.

A key consideration in implementing the WMD-EWMA control chart is the selection of the window length, which benefits from prior knowledge about the specific characteristics of the monitored process. With appropriate contextual knowledge, selecting a window length is straightforward: shorter windows provide greater responsiveness but may increase false positives from post-drift fluctuations, while longer windows reduce false alarms at the cost of delayed detection. This trade-off is manageable when practitioners have reasonable expectations about drift frequency and process dynamics, allowing the chart's performance to be aligned with operational requirements.

In conclusion, the WMD-EWMA control chart represents a significant enhancement over existing methods, offering a powerful and efficient solution for detecting large mean drifts in autocorrelated data, making it the preferred choice for quality control and process monitoring in complex, real-world scenarios.

5 | Recommendation and Future Work

The WMD-EWMA chart is highly recommended for applications where detecting large mean drifts is critical, such as in manufacturing quality control, network performance monitoring, or environmental monitoring. Its ability to reduce false positives while accurately detecting drifts makes it an ideal tool in these contexts. To maximise the effectiveness of the WMD-EWMA method, careful consideration should be given to the selection

of the window length parameter, which should be tailored to the specific characteristics of the data being monitored. Practitioners should take into account the nature of the process noise, the frequency of expected drifts and the operational context when setting this parameter.

The WMD-EWMA chart proves to be effective even in processes without significant mean drifts. While this study confirms the robustness of the WMD-EWMA chart in drift detection, there are several avenues for future research. These include exploring adaptive window lengths that adjust based on process behaviour, incorporating run rules to improve the detection of subtle changes, integrating the chart with machine learning models to enhance predictive capabilities and periodically re-estimating control limits to ensure ongoing reliability and minimise false alarms in complex, non-stationary environments. Additionally, expanding the application of the WMD-EWMA chart to high-dimensional datasets and conducting long-term evaluations across diverse industries such as finance, healthcare and industrial control could further validate its effectiveness and generalisability.

Acknowledgement

The first author expresses gratitude to the South African Medical Research Council (SAMRC) for their generous funding, which has made this research possible. This support was provided through the Division of Research Capacity Development as part of the SAMRC Biostatistics Capacity Development Initiative. It is important to note that the views expressed in this article are solely those of the authors and do not necessarily represent the official stance of the SAMRC or its funding partners.

Data Availability Statement

The data are available on request from the authors.

References

1. S. B. Kim, W. Jitpitaklert, S.-K. Park, and S.-J. Hwang, "Data Mining Model-Based Control Charts for Multivariate and Autocorrelated Processes," *Expert Systems with Applications* 39, no. 2 (2012): 2073–2081, https://doi.org/10.1016/j.eswa.2011.08.010.

2. L. Xue, Q. Wang, L. An, Z. He, S. Feng, and J. Zhu, "A Nonparametric Adaptive EWMA Control Chart for Monitoring Mixed Continuous and Categorical Data Using Self-Starting Strategy," *Computers & Industrial Engineering* 188 (2024): 109930, https://doi.org/10.1016/j.cie.2024.109930.

3. D. C. Montgomery, *Introduction to Statistical Quality Control* (John Wiley & Sons, United States of America, Inc, 2009).

4. Y. Lima de Mendonca, R. Sarto, H. Titeca, R. Bethune, and A. Salmon, "Use of Statistical Process Control in Quality Improvement Projects in Abdominal Surgery: A PRISMA Systematic Review," *BMJ Open Quality* 13 (2024): e002328, https://doi.org/10.1136/bmjoq-2023-002328.

5. B. Y. Wotango, T. D. Abdana, H. Kidane, E. B. Jote, G. T. Simeneh, and W. M. Workneh, "Using Control Charts to Understand Variation: A Tool for Process Improvement in Healthcare," *Global journal on quality and safety in healthcare* 8, no. 3 (2025): 141–143, https://doi.org/10.36401/JQSH-25-2.

6. W. A. Shewhart, "Economic Control of Quality of Manufactured Product," *Bell System Technical Journal* 9, no. 2 (1930): 364–389, https://doi.org/10.1002/j.1538-7305.1930.tb00373.x.

7. S. Roberts, "Control Chart Tests Based on Geometric Moving Averages," *Technometrics* 1 (1959): 239–250, https://doi.org/10.1080/00401706.1959.10489860.

8. A. Kurtulus, D. Goossens, and D. van Bulck, *Control Charts for Monitoring Processes With Autocorrelated Data* (Tesis de Fin de Master, Universidad de Gante, 2020). Ph.D. thesis.

9. R. Ramjee, N. C. Bonnie, and K. Ray, "A Note on Moving Average Forecasts of Long Memory Processes With an Application to Quality Control," *International Journal of Forecasting* 18, no. 2 (2002): 291–297, https://doi.org/10.1016/S0169-2070(01)00159-5.

10. D. C. Montgomery and C. M. Mastrangelo, "Some Statistical Process Control Methods for Autocorrelated Data," *Journal of quality technology* 23, no. 3 (1991): 179–193, https://doi.org/10.1080/00224065.1991.11979321.

11. A. Chen and Y. K. Chen, "Design of EWMA and CUSUM Control Charts Subject to Random Shift Sizes and Quality Impacts," *IIE Transactions* 39, no. 12 (2007): 1127–1141, https://doi.org/10.1080/07408170701315321.

12. Z. Mou, J. Y. Chiang, S. Chen, and G. Liu, "A Likelihood-Based Adaptive CUSUM for Monitoring Linear Drift of Poisson Rate With Time-Varying Sample Sizes," *Journal of Statistical Computation and Simulation* 94, no. 10 (2024): 2210–2235, https://doi.org/10.1080/00949655.2024.2327376.

13. M. J. Zhao, A. R. Driscoll, S. Sengupta, R. D. Fricker Jr, D. J. Spitzner, and W. H. Woodall, "Performance Evaluation of Social Network Anomaly Detection Using a Moving Window-Based Scan Method," *Quality and Reliability Engineering International* 34, no. 8 (2018): 1699–1716, https://doi.org/10.1002/qre.2364.

14. Y. Wang, G. Huang, J. Yang, et al., "Change Point Detection With Mean Shift Based on AUC From Symmetric Sliding Windows," *Symmetry* 12, no. 4 (2020): 599, https://doi.org/10.3390/sym12040599.

15. D. Mejri, M. Limam, and C. Weihs, "A New Time-Adjusting Control Limits Chart for Concept Drift Detection," *IFAC Journal of Systems and Control* 17 (2021): 100170, https://doi.org/10.1016/j.ifacsc.2021.100170.

16. F. Yi, and P. Qiu, M. Abid, and I. A. Arshad, "An Adaptive CUSUM Chart for Drift Detection," *Quality and Reliability Engineering International* 38 (2022): 887–894, https://doi.org/10.1002/qre.3020. 2022.

17. J. De Smedt, A. Yeshchenko, A. Polyvyanyy, J. De Weerdt, and J. Mendling, "Process Model Forecasting and Change Exploration Using Time Series Analysis of Event Sequence Data," *Data & Knowledge Engineering* 145 (2023): 102145, https://doi.org/10.1016/j.datak.2023.102145.

18. R. A. Fisher, "The Use of Multiple Measurements in Taxonomic Problems," *Annals of Eugenics* 7, no. 2 (1936): 179–188, https://doi.org/10.1111/j.1469-1809.1936.tb02137.x.

19. R. Gontier, J. Deverge, M. Schoenauer, and V. D. Blondel (2021). Time evaluation datasets, Accessed: 2024-08-29. https://timeeval.github.io/evaluation-paper/notebooks/Datasets.html.

Appendix A

In Equation (3), the IMA (1,1) model was defined as

$$X_t = X_{t-1} + a_t - \theta a_{t-1}. \tag{A1}$$

The optimal one-step-ahead forecast $\hat{X}_t(t-1)$ is the expectation of X_t given all information up to time $t-1$. Then, $\hat{X}_t(t-1)$ becomes

$$\begin{aligned}\hat{X}_t\,(t-1) &= E\,(X_t|X_{t-1}, X_{t-2}, \ldots)\\ &= E\,(X_{t-1} + a_t - \theta a_{t-1}|X_{t-1}, X_{t-2}, \ldots)\\ &= X_{t-1} - \theta a_{t-1}\end{aligned}$$

Thus,

$$\hat{X}_t\ (t-1) = X_{t-1}\ - \theta a_{t-1}. \tag{A2}$$

Substituting Equations (A1) and (A2) into Equation (5):

$$E_t = a_t \tag{A3}$$

Substituting Equation (A3) into (A2), we get

$$\hat{X}_t\ (t-1) = X_{t-1}\ - \theta E_{t-1}. \tag{A4}$$

Substituting Equation (5) into (A4) and setting $\lambda = 1-\theta$, then $\hat{X}_t(t-1)$ becomes

$$\hat{X}_t\ (t-1) = \lambda\, X_{t-1} + (1-\lambda)\ \hat{X}_{t-1}\,(t-2)\,. \tag{A5}$$

Equation (1) and (A5) are equivalent only when

$$\hat{X}_t\ (t-1) = Z_{t-1}\,. \tag{A6}$$

Appendix B

This appendix presents the in-control run-length (RL_0) distributions and its properties ($ICARL$, $SDRL_0$, fifth, $50^{th,}$ 75^{th} and 95^{th} PRL_0) found using the datasets under consideration, that is D_1, D_2, D_3 and D_4 when $ARL_0 = 350$.

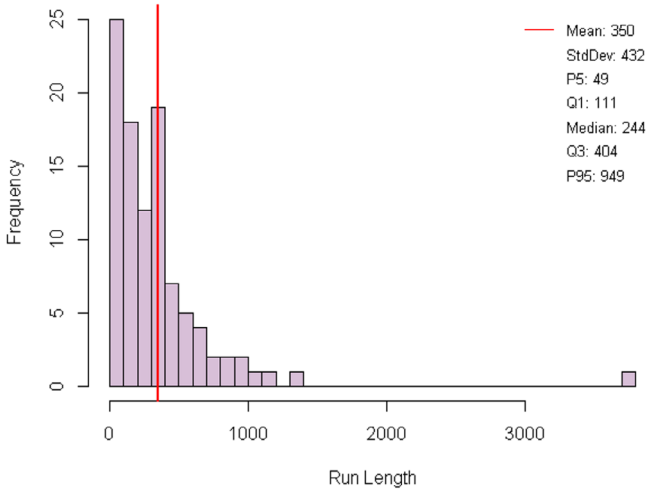

FIGURE B1 | Properties of the RL_0 distribution for D_1.

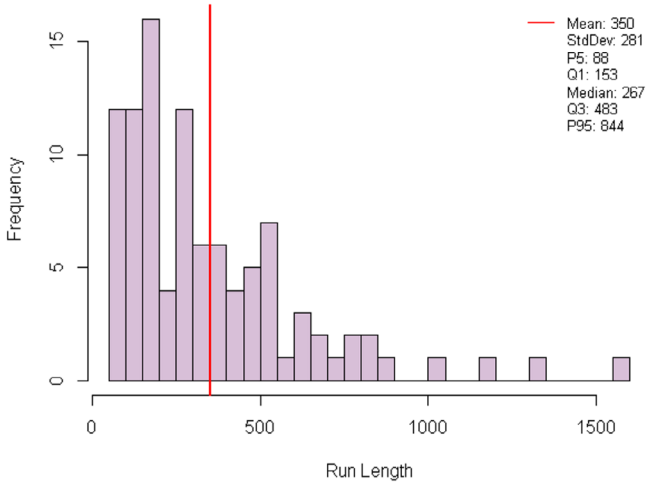

FIGURE B2 | Properties of the RL_0 distribution for D_2.

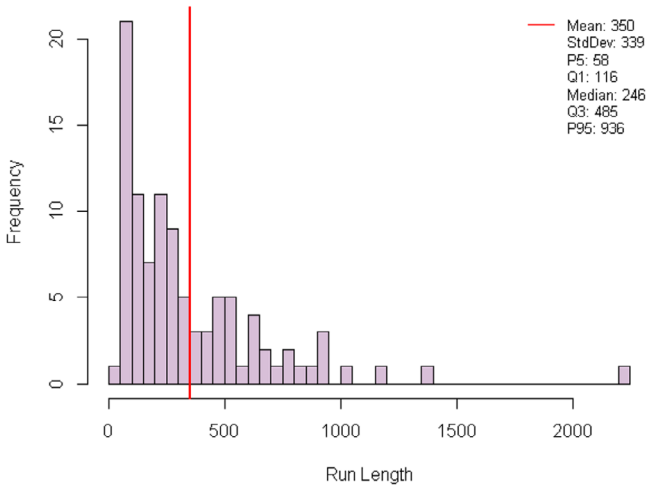

FIGURE B3 | Properties of the RL_0 distribution for D_3.

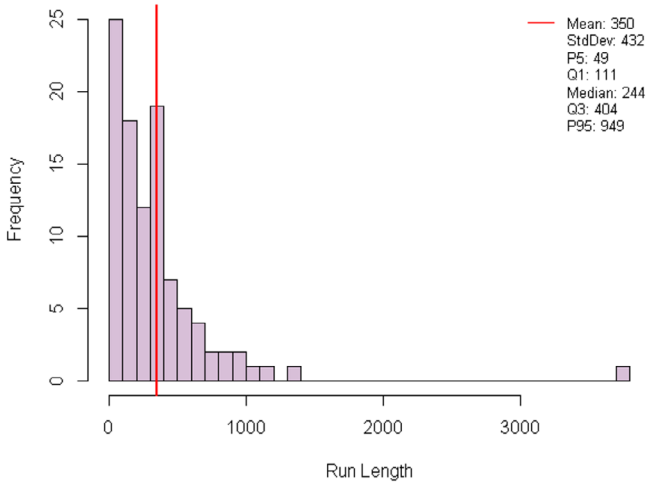

FIGURE B4 | Properties of the RL_0 distribution for D_4.